Int J Clin Exp Pathol 2019;12(2):443-454
www.ijcep.com /ISSN:1936-2625/IJCEP0088831

Original Article

Morphologic and histopathologic change of sodium iodate-induced retinal degeneration in adult rats

Yang Liu, Ying Li, Chenguang Wang, Yinan Zhang, Guanfang Su

Eye Center, The Second Hospital of Jilin University, Changchun, Jilin, China

Received November 23, 2018; Accepted December 18, 2018; Epub February 1, 2019; Published February 15, 2019

Abstract: Adult teleost fish are capable of regenerating their retinas following injury. In contrast, the adult mammalian retina has little capacity for regeneration. Here, we describe the morphologic and histopathologic course of sodium iodate ($NaIO_3$) injection on rat retinas. A single dose of $NaIO_3$ (50 mg/kg) was administered intravenously to adult Sprague-Dawley male rats. Control animals received sodium chloride. Morphologic and molecular changes following $NaIO_3$ injection were monitored by histological and gene expression analysis. We observed retinal pigment epithelium (RPE) cell death began at 6 h PI. After 3 and 7 days, we found local tissue repair by RPE cell regeneration. This was further confirmed by a significant decrease in photoreceptor cell apoptosis in the outer nuclear layer. Protein-level analysis demonstrated the attenuated regulation of cellular markers specially related to active gliosis in retinal Müller cells, including cellular retinaldehyde-binding protein (CRALBP) and glutamine synthetase (GS), after $NaIO_3$ treatment for 3rd and 7th days. The Müller cells exhibited signs of dedifferentiation, as paired box 6 (PAX6) and SRY box 2 (SOX2) were expressed by $NaIO_3$ stimulated Müller glia proliferation and overexpression of proliferating cell nuclear antigen (PCNA). We concluded that $NaIO_3$ injection can result in significant and progressive damage to RPE and photoreceptor cells. Our observations suggest that Müller cell transient differentiation and RPE recovery is induced in the mammalian retina by relatively high doses of $NaIO_3$. Transient change in Müller cell differentiation and RPE cell recovery may result in photoreceptor apoptosis decrease.

Keywords: Müller cell, retinal pigment epithelial cell, $NaIO_3$, differentiation

Introduction

Age-related macular degeneration (AMD) is a degenerative disease characterized by photoreceptor and retinal pigment epithelium (RPE) impairment in the human macula, resulting in irreversible visual loss [1]. The introduction of anti-vascular endothelial growth factor (VEGF) therapy has enabled prominent advances in the management of exudative or wet AMD [2-4]. While this has revolutionized AMD outcomes, anti-VEGF agents must be administered repeatedly, sometimes monthly, over long periods. Furthermore, these treatments are expensive, and in many countries are not accessible to all patients. The development of additional effective therapeutic strategies requires comprehensive elucidation of the biological processes underlying AMD.

Systematic delivery of sodium iodate ($NaIO_3$), which selectively destroys the RPE and elicits AMD-associated features, has been widely used to understand the mechanisms involved in retina degeneration and regeneration [5-7]. In animal models, $NaIO_3$-induced structural and functional changes are time- and dose-dependent [8, 9]. As $NaIO_3$ is a stable oxidizing compound, the initiation and progression of degeneration may be modulated, facilitating the design of potential therapeutic approaches to regenerate the damaged RPE [10, 11]. Machalinska et al. demonstrated that RPE regeneration occurs following low-dose $NaIO_3$ (40 mg/kg body weight)-induced retinal degeneration [12]. Until recently, few studies have reported endogenous retinal repair following rapid RPE damage induced by relatively high doses of $NaIO_3$ (50-100 mg/kg).

To date, no reports have specifically assessed the effect of $NaIO_3$ on endogenous retinal regeneration. The aim of the present study was to elucidate endogenous RPE regeneration

after damage with a high dose of $NaIO_3$ (50 mg/kg). Here, we present a systematic histological and molecular analysis of the effects of experimental retinal injury with a relatively high dose of $NaIO_3$ through a long observational period. The purpose of this study was to explore and identify the morphologic and histopathologic course involved in retinal regeneration by detecting specific gene expression changes after $NaIO_3$ treatment.

Methods

Animals and ethical considerations

Adult male Sprague-Dawley rats (weighing 280-300 g) were purchased from the Medical Center of Jilin University. The study was approved by the Second Hospital of Jilin University Ethics Committee. All animal experiments complied with the Association for Research in Vision and Ophthalmology Statement for the Use of Animals in Ophthalmic and Vision Research and were approved by the local ethics committee. The operational procedure followed the European Union Directive 2010/63/EU on the protection of animals used for scientific research. Rats were housed in a standard laboratory environment with a 12-hour light-dark cycle and unlimited access to food and water. Anesthesia performed by intraperitoneal injection with ketamine (120 mg/kg) (Hengrui Medicine, China) and xylazine (5 mg/kg) (Sigma, USA). Animals were euthanized by cervical dislocation under anesthesia when the eyeballs were removed at the end of the experimental phase of the study. We ensure the animal welfare and complied with the 3R principle prior to, during, and after the experiments.

Treatment with $NaIO_3$

Seventy animals were divided into $NaIO_3$-treated and control groups. Sterile 1% $NaIO_3$ (Sigma-Aldrich, St. Louis, USA) diluted in 0.9% NaCl freshly before injection. The rats were injected with 50 mg/kg body weight $NaIO_3$ once by the tail vein and examined for 28 days post-injection (PI). Control rats received a single intravenous injection of 0.9% NaCl.

Histologic assessment of the retina

The eyes were harvested at 6 hours, 1, 3, 7, 14 and 28 days after injection of $NaIO_3$ under anesthesia. Eyeballs were fixed with 4% paraformaldehyde in phosphate-buffered saline (PBS) for 30 minutes at room temperature. Samples were embedded in Optimum Cutting Temperature Compound (O.C.T., USA), sectioned at a thickness of 5 μm through the optic nerve head, and mounted on glass slides. The frozen sections were stained with hematoxylin and eosin (H&E-stained) and embedded on dehydrated slides in mounting medium. Magnified images (200×) were captured using a light microscope (BX51, Olympus, Japan) connected to a Spot digital camera (DP72, Olympus, Japan). Analyzed retinal sections were captured in the same site, located in the optic nerve head.

Immunohistochemistry

Prepared frozen retinal sections were washed with PBS and 0.2% Triton X-100 in PBS for 15 minutes at room temperature. Samples were incubated in a blocking buffer containing 1% normal goat serum, then primary antibodies were added for overnight incubation at 4°C. All primary antibodies were from Abcam, and were diluted as follows: anti-cellular retinal-binding protein (CRALBP, 1:50), anti-paired box 6 (PAX6, 1:50), anti-glutamine synthetase (GS, 1:200), anti-SRY box 2 (SOX2, 1:50), anti-proliferating cell nuclear antigen (PCNA, 1:50), and anti-RPE65 (RPE65, 1:100). Sections were washed with PBS and incubated with secondary antibodies for 1 hour at 37°C. Cell nuclei were stained with 4',6-diamidino-2-phenylindole (1:600, Beyotime). Secondary antibodies, including goat anti-mouse Alexa Fluor 488 (1:600, Thermo) and goat anti-rabbit Cy3 (1:800, Thermo), were diluted in 1% bovine serum albumin. Images were acquired using an Olympus microscope.

Western blot analysis

After treatment with $NaIO_3$, retinas were extracted in presence of lysis buffer and protease inhibitor (Thermo, USA) for 30 minutes and centrifuged at 12,000×g (Legend Micro 17R, Thermo, USA) for 10 minutes at 4°C. The supernatant was collected and the total protein content was quantified using a BCA Protein Assay Kit (Beyotime, China), following the manufacturer's protocol. Equal amounts of protein (10 μl, 30 μg) were separated by 10% sodium

dodecyl sulfate-polyacrylamide gel electrophoresis, and transferred onto polyvinylidene difluoride membranes at 50 or 70 V for 100 minutes at 4°C. The membranes were blocked using 5% non-fat milk for 2 hours at room temperature. Primary antibodies, including mouse anti-CRALBP (1:3,000, Abcam), mouse anti-GS (1:3,000, Abcam), rabbit anti-PAX6 (1:1,000, Abcam), rabbit anti-SOX2 (1:1,000, Abcam), and mouse monoclonal anti-RPE65 (1:500, Abcam) and mouse anti-beta actin-loading control (1:1,000, CMCTAG, USA) were diluted in blocking buffer for addition to the membranes, which were then incubated at 4°C overnight. Next, the membranes were incubated with goat anti-rabbit or mouse secondary antibody conjugated to horseradish peroxidase (1:5,000, BosterBio, China) for 1.5 hours at room temperature. The membranes were washed thrice after incubation with primary antibodies and secondary antibodies with T-BST buffer (15 min one time). Protein signals were detected using an enhanced chemiluminescence system (DNR MF-ChemiBIS 3.2) and the band density was measured using ImageJ public domain software (W.S. Rasband, ImageJ, U.S. National Institutes of Health).

Terminal deoxynucleotidyl transferase (TdT) dUTP nick-end labeling (TUNEL) assay

Prepared retinal histological sections were stained using a TdT In Situ DAB in situ Apoptosis Detection Kit (Roche Diagnostics GmbH, Mannheim, Germany), according to the manufacturer's instructions. Specimens were examined under a light microscope (Olympus, Japan).

Statistical analysis

All experiments were repeated in triplicate. Quantitative data are presented as the mean ± standard error of the mean. Statistical Package for Social Science (SPSS) 17.0 software was used for analysis. Statistical analysis was performed using Student's t test or one-way analysis of variance followed by t test, using the Bonferroni correction for multiple comparisons. Differences between groups were considered-significant at $P < 0.05$.

Results

Histological data

H&E-stained retinal sections from the same locations from optic disks treated with a 50 mg/kg dose were displayed (**Figure 1**). A healthy retina at baseline showed all layers found in normal rat retina (**Figure 1A**). $NaIO_3$-treated retinas at different stages PI (**Figure 1B-G**) presented disruption of the OS layer (gray arrow) and the formation of gaps between the OS and RPE (black arrow) were evident 6 h PI, and early changes involving RPE nuclear disintegration occurred (**Figure 1B**). After 1 day PI, RPE injury was already evident, and it was difficult to identify the cell nuclei. In addition, swelling and disorganization of IS/OS photoreceptors occurred (**Figure 1C**). On 3rd day (**Figure 1D**), cell migration (possibly host macrophages, black arrows) between the OS and the RPE layer was observed. Over the ensuing 7-14 days (**Figure 1E**, **1F**), the RPE monolayer was destroyed, subsequently, the layers of the neural retina were also altered compared with the control. The RPE cell nuclear disintegration and loss of infoldings on the basal membrane, disappearance apical microvilli and tight junctions were observed. At 28 days PI (**Figure 1G**), the RPE layer was largely absent, with only a few discontinuous and disorganized rows of photoreceptor nuclei present; and the IS/OS were not maintained.

To quantify the changes in the neurosensory retina, we measured the thickness of the two outer retinal layers (INL, ONL, and IS/OS) and the numbers of nuclei rows in the INL and ONL in the H&E stained cross sections between 6 h PI and 28 days PI (**Figure 1H**). At 6 h and 1 day PI, measurements of the inner and outer segments (IS/OS) were mildly increased due to swelling and no statistically significant difference from the control was observed on 3rd day PI. However, this was temporary; these changes were progressive over time PI, accompanied by the thickness of the ONL, which began to reduce at 7th day PI and significantly decreased on 28th day PI (**Figure 1H**). This decline in ONL thickness and the number of photoreceptor nuclei rows may be due to soma shrinkage and apoptosis. The thickness of the inner retinal layer (INL) was also calculated; however, no obvious changes were detected between the treated and control groups (**Figure 1I**).

Effect of $NaIO_3$ on RPE65 expression in rat RPE monolayer

To investigate whether acute chemical injury has a noticeable impact on RPE monolayer, we

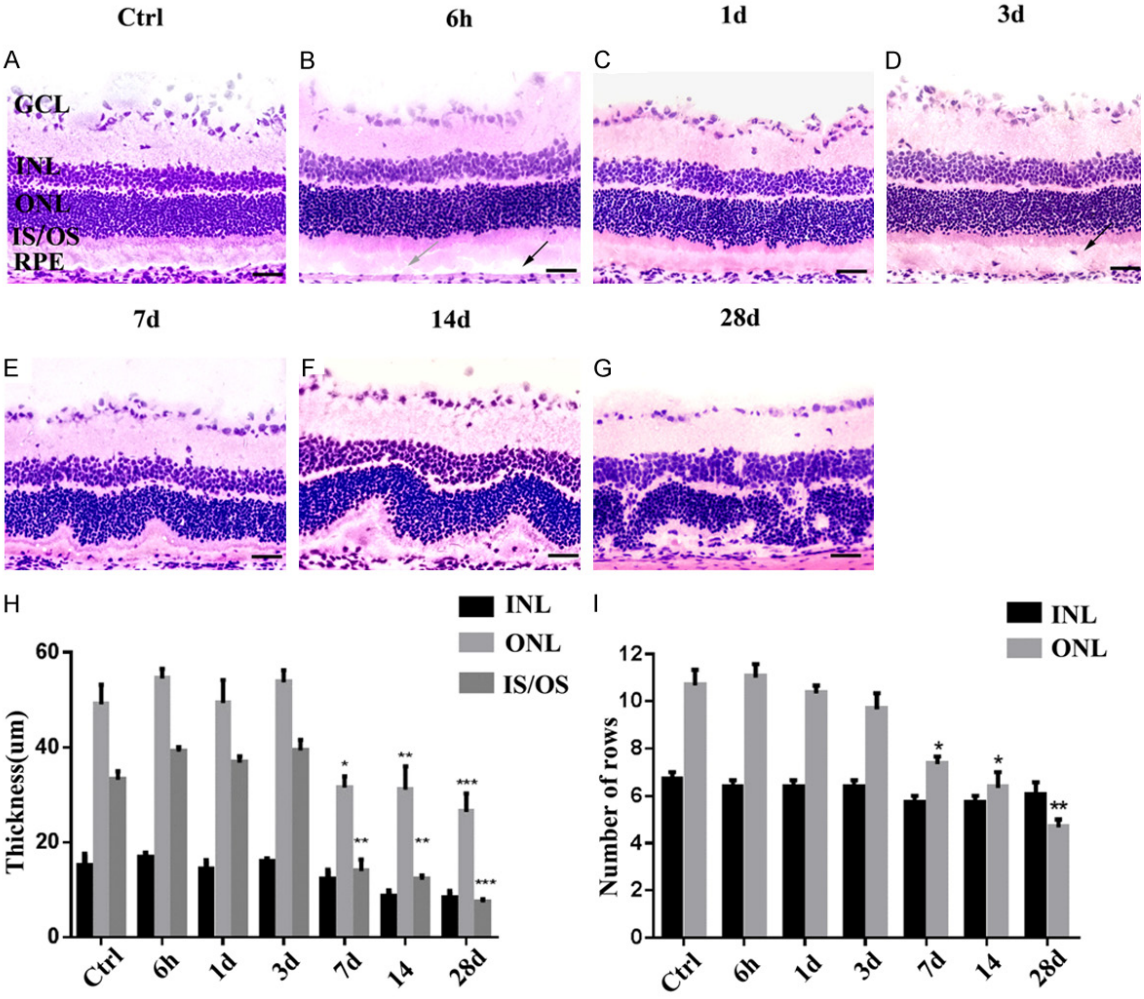

Figure 1. H&E staining to assess retinal injury after $NaIO_3$ treatment (A-G). Over time, the RPE monolayer was destroyed and subsequently, the layers of the neural retina were also altered. A comparison of retinal thickness (μm; mean ± SD, n = 5) at subsequent time points after $NaIO_3$ administration were quantitated in each photomicrograph in the following retinal layers: INL, ONL, and OS (H). The number of rows was counted manually in pictures taken at three equal distances from the optic disk. Graphs showing the mean (± SD) numbers of nuclei rows in the INL and ONL of control and treated groups (I). (*P < 0.05, **P < 0.005, ***P < 0.0010). GCL, ganglion cell layer; INL, inner nuclear layer; ONL, outer nuclear layer; IS/OS, inner and outer segment; RPE, retinal pigment epithelium. Scale bar, 100 μm.

next monitored the destruction process of RPE cells induced by $NaIO_3$ and examined the intensity of local tissue repair by RPE regeneration (**Figure 2**). Systemically administered $NaIO_3$ resulted in a rapid destruction of RPE cells in injured retinas at 6 h PI compared with controls, as evidenced by histological evaluation (**Figure 2A**, **2B**). The epithelial monolayer was completely disrupted, and individual RPE cells showed multiple phenotypes after 1 day injection (**Figure 2C**). Although the RPE cells were multilayered in some areas, complete regeneration of the RPE structure at the sites of injury could be observed. Notably, similar to the control, the flattened scattered RPE cells indicated regeneration of the RPE structure at the sites of injury (**Figure 2D**, **2E**). Furthermore, the RPE monolayer was disrupted, and RPE cells were occasionally observed (**Figure 2F**, **2G**)

In our continuing efforts to characterize the retinal regenerative response to chemical injury, we analyzed whether the RPE65 aggregated in the retina following $NaIO_3$ injection. Western

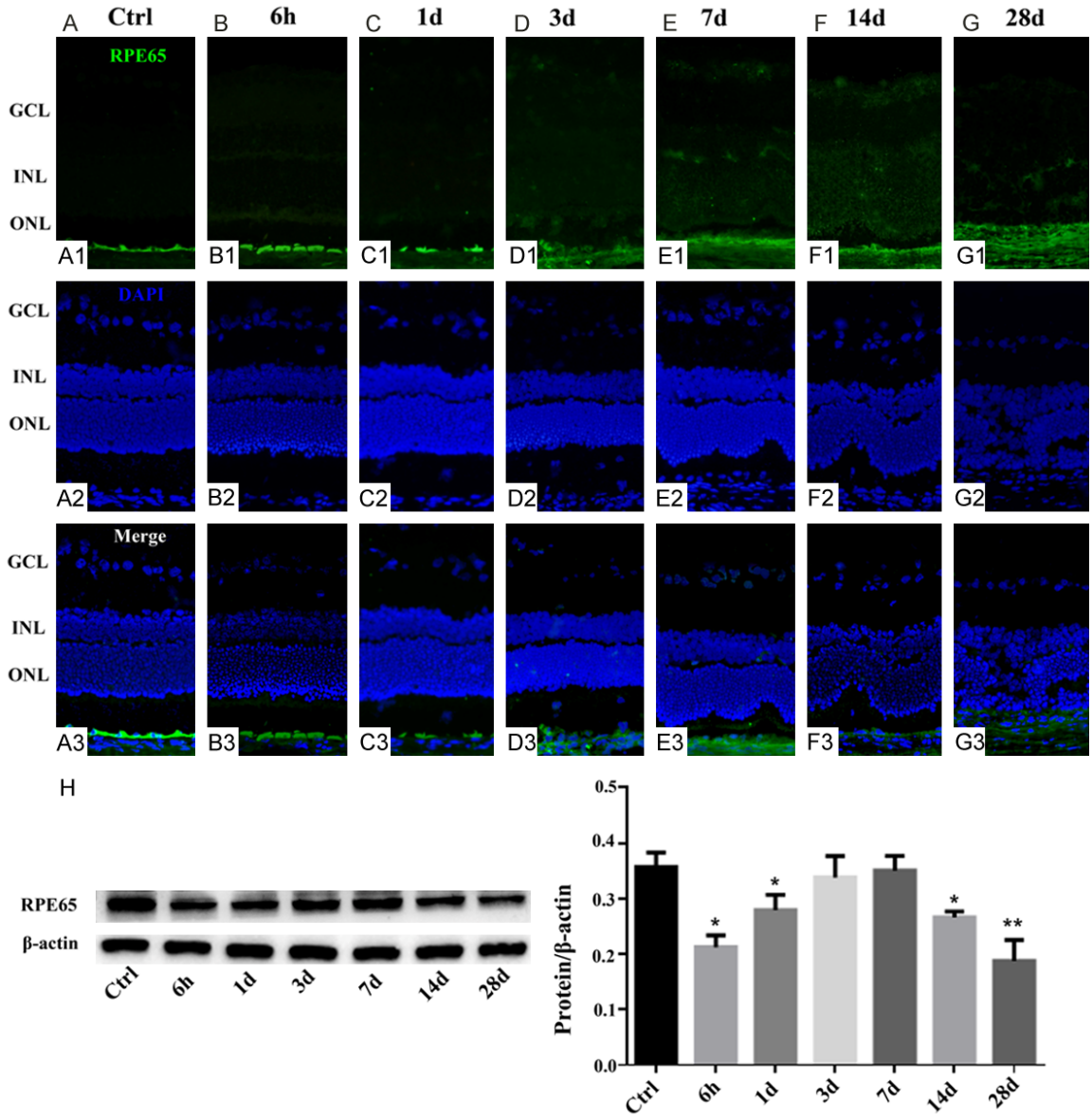

Figure 2. Effect of $NaIO_3$ on RPE65 expression in the RPE cells in retinas. Immunocytochemical staining for RPE65 in the retinas of $NaIO_3$-treated and control rats. Control healthy retina with no signs of injury (A). The RPE cell was degenerated at 6 h post $NaIO_3$ injection (B), and this was particularly obvious at 1 day PI (C). Histological assessment of the retinas at 3-7 days PI revealed regeneration of the RPE structure at the sites of injury (D, E). Then the remaining RPE structure could not be detected indicating direct signs of local injury to the RPE (F, G). Western blotting was used to confirm RPE65 expression in the groups (H). The graph shows the ratio of RPE65 to β-actin in each group. RPE65 expression was reduced in other $NaIO_3$ group but increased significantly 3 and 7 days PI (*, $P < 0.05$; **, $P < 0.005$).

blot analysis confirmed that the RPE65 degenerated compared with the control healthy retina at 6 h and lasted 1 day after injection (**Figure 2H**). Similar injury-related recovery trends were observed at 3rd and 7th day PI, as confirmed by immunochemical staining. Western blot analysis confirmed prominent RPE65 upregulation after 3 and 7 days PI, which gradually declined afterwards and persisted at a very low level until the end of the experiment. This result may indicate that RPE cells possess the capacity for reorganization and transient regeneration.

$NaIO_3$ induces apoptosis in photoreceptor cells

To follow the kinetics of the RPE recovery process, we next investigated photoreceptor cell death in $NaIO_3$-treated and control retinas. The

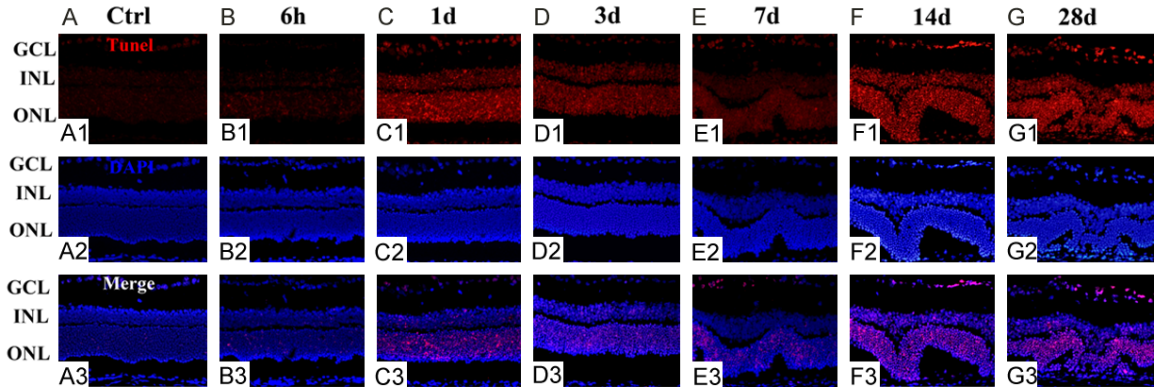

Figure 3. $NaIO_3$ induces photoreceptor cell apoptosis. A TUNEL assay (red) was performed on control and $NaIO_3$ retinas. DAPI (blue) was used to stain the nuclei. The extent of photoreceptor cell death in retinas treated with $NaIO_3$ was comparable to that in control retinas. No TUNEL-positive cells were found in the ONL of the control samples (A). TUNEL-positive photoreceptors (red) were detected at 6 h post-injection and persisted until day 1 (B, C). TUNEL-positive RPE cells appeared attenuated at days 3 and 7 (D, E). The number of TUNEL-positive cells increased until 14th and 28th day PI, indicating that the cells were undergoing apoptosis (F, G).

time courses of the changes related to photoreceptor cell death in control and at different time points after $NaIO_3$ injection are summarized in **Figure 3**. TUNEL-positive cells were absent in the control sections (**Figure 3A**) but were detectable starting from 6 h PI and were rather obvious at 1 day PI (**Figure 3B**, **3C**). TUNEL-positive cells (red) were restricted to the outer nuclear layer (ONL), in which the photoreceptor nuclei are located, indicating a cell-specific effect of $NaIO_3$ administration. TUNEL positivity decreased over time (**Figure 3D**, **3E**), indicating that photoreceptor degeneration is rather slow to progress after $NaIO_3$ damage. Moreover, TUNEL positivity in retinal sections was significantly upregulated compared with that of the controls at 14th day PI, which persisted until the 28th day (**Figure 3F**, **3G**).

Effects of $NaIO_3$ on Müller cell proliferation in the INL

To assess cell proliferation after $NaIO_3$ treatment, we stained sections for PCNA at the same time points as those used in H&E staining and observed proliferation in the INL. To determine whether the observed proliferation resulted from Müller cells, sections of retinas were co-labeled with antibodies against CRALBP and GS. PCNA immunoreactivity was detected in the control retinas (**Figure 4A1**, **4A2**) and the reactivity was attenuated in the Müller cells after exposure to $NaIO_3$ at 6 h and 1th day (**Figure 4B1**, **4C1**, **4B2**, **4C2**). At 3 days after damage, when the appearance of PCNA reached the peak level as detected by immunofluorescence, colocalization with CRALBP- and GS-positive cells in the INL was observed, and the PCNA expression was maintained until the 7th day (**Figure 4D1**, **4E1**, **4D2**, **4E2**). Subsequently, PCNA immunoreactivity did not overlap with CRALBP and GS staining in the INL following $NaIO_3$ treatment (**Figure 4F1**, **4G1**, **4F2**, **4G2**).

Similar to the patterns of expression detected by immunofluorescence, retinas were stained using primary antibodies against PCNA. Increased PCNA levels were observed 3 and 7 days after $NaIO_3$ treatment (**Figure 4H**). No statistically significant changes in expression were noted between the control and other damaged retinas. As CRALBP and GS are markers of retinal Müller cells, we probed for changes in CRALBP and GS levels in retinas treated with $NaIO_3$. We found that $NaIO_3$ inhibited Müller cell glial reactivity, and CRALBP and GS levels were significantly reduced at 3rd and 7th day PI in damaged retinas compared to control retinas. These results suggest that $NaIO_3$ treatment-induced cell proliferation in the INL of the retinas was attributable to Müller cells.

Müller cell showed upregulated SOX2 and PAX6 expression following retinal damage

To verify that proliferative Müller cells in the INL undergo dedifferentiation, PAX6, and SOX2

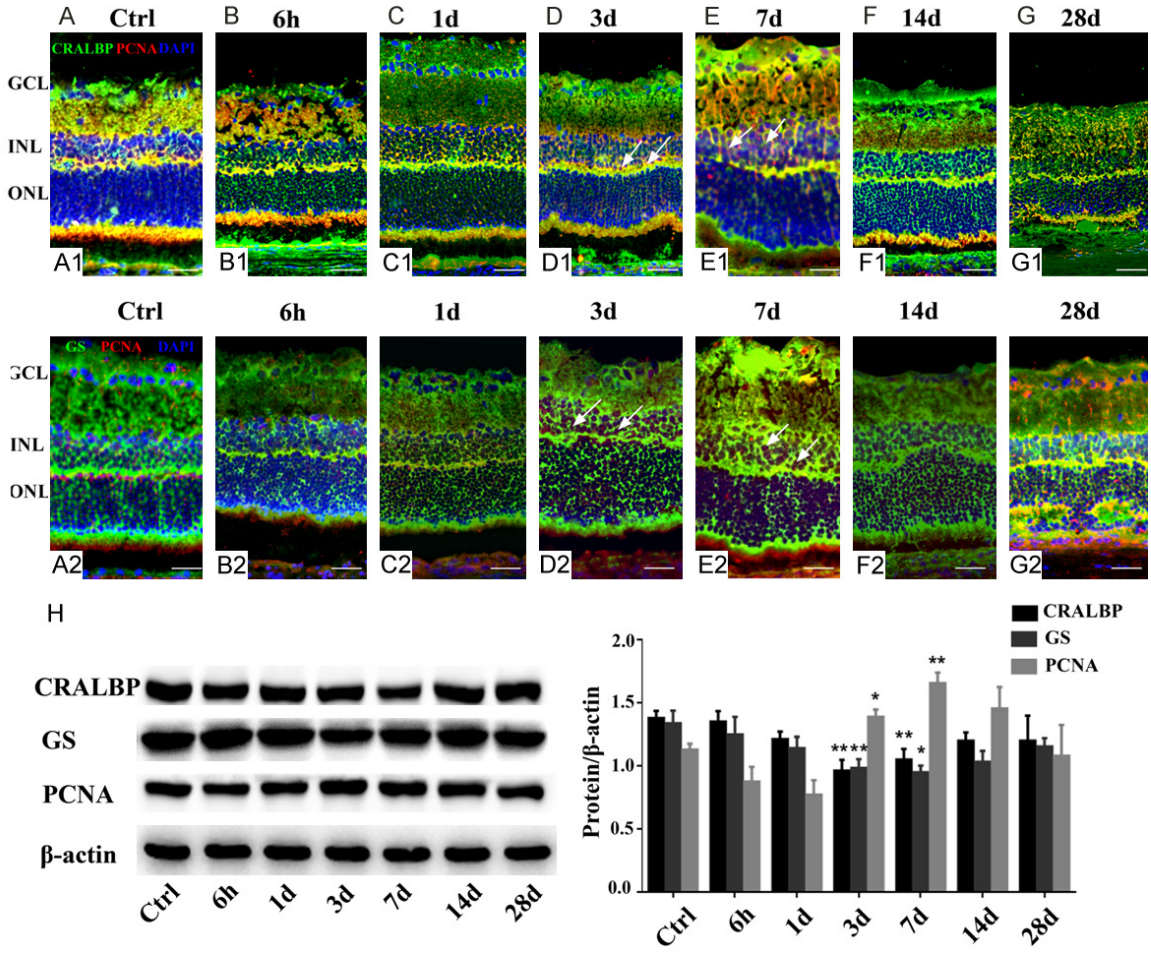

Figure 4. Müller cell proliferation in rat retinas treated with $NaIO_3$ (A-G). (A1-G1) Representative photographs of immunofluorescence with anti-PCNA (red) and anti-CRALBP (green) (upper panels). (A2-G2) Representative photographs of immunofluorescence with anti-PCNA (red) and anti-GS (green) (lower panels). Proliferating cell nuclear antigen (PCNA)-positivity (red) represents proliferation. When compared with the control (A1, A2), few PCNA-positive nuclei were detected in the INL after 6 h and 1 day post $NaIO_3$-treament (B1 and C1, B2 and C2). Arrows indicate the colocalization of PCNA (red) with CRALBP or GS (green), suggesting that Müller cell proliferation significantly increased at 3-7 days following $NaIO_3$ injection *in vivo* (D1 and E1, D2 and E2). At (F1 and F2), $NaIO_3$-treated retinas exhibited limited number of a-PCNA expressing cells. In (G1 and G2), very few PCNA-positive cells were found to undergo proliferation in the INL, as assessed by immuno-double labeling. Western blot analysis showed the expression of Müller cell markers (H). CRALBP and GS were detected at all time points, and their levels decreased significantly, whereas the expression of PCNA increased in the retinal tissues after 3 and 7 days PI compared with the control. Significant differences were determined using Student's *t*-test (*, $P < 0.05$; **, $P < 0.005$).

(dedifferentiation markers) were detected by immunofluorescence of frozen retinal sections co-stained for either CRALBP and PAX6 or GS and SOX2. $NaIO_3$-treatment of the retinas had no effect on the up-regulation of nuclear PAX6 and SOX2 *in* Müller cells at 6 h and 1 day compared to the levels seen in the nuclei of Müller cell in the uninjured retinas (**Figure 5A1-C1**, **5A2-C2**). At sequential time points after injury induction, we found a significant increase in neuronal differentiation on 3rd and 7th day. Compared to control retinas, there was significant increase in the percentage of PAX6- and SOX2-positive cells labeled for the neuronal markers CRALBP and GS in the INL of $NaIO_3$-treated retinas (**Figure 5D1**, **5E1**, **5D2**, **5E2**). However, similar to the change of PCNA immunoreactivity, there was a observable decrease in the numbers of PAX6- and SOX2-positive cells at 14th day, and this decrease lasted until the 28th day (**Figure 5F1**, **5G1**, **5F2**, **5G2**). Cells that accumulated PAX6 and SOX2 in the INL

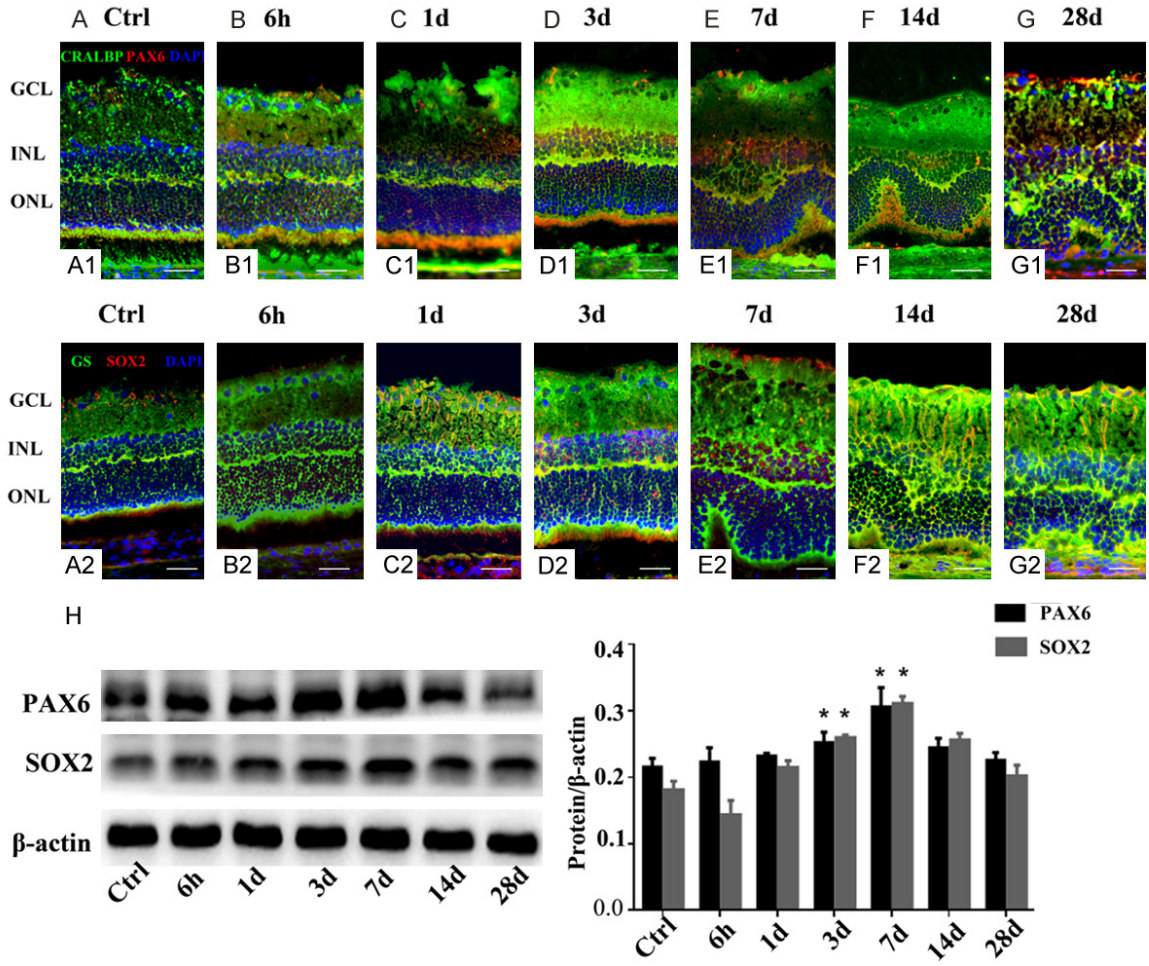

Figure 5. Effect of $NaIO_3$ on PAX6 and SOX2 expression in the Müller cells of rat retinas (A-G). Double-stained CRALBP and PAX6 (A1 and G1) or GS and SOX2 (A2 and G2) sections were used to visualize dedifferentiated glial cells within the INL of the retina. Control retina with no sign of injury (A1, A2). The ratio of PAX6- and SOX2-positive cells was similar at 6 h and 1 day PI, when compared with the control (B1 and C1, B2 and C2). The percentages of positive cells were high on 3rd and 7th day PI, showing a cluster of PAX6- and SOX2-positive cells (D1 and E1, D2 and E2). Images (F1 and F2) show that only some cells exhibited weak reactivity, and no expression of dedifferentiation markers was detected (G1, G2). Pseudocolors were assigned to each staining as follows: CRALBP and GS, green; PAX6 and SOX2, red; nuclei, blue. Western blot (H) was used to analyze differences in PAX6 and SOX2 protein expression between $NaIO_3$-treated and control retinas; the histogram shows significantly increased expression of SOX2 and PAX6 in retinas harvested after 3 and 7 days PI. (*, $P < 0.05$).

were Müller cells, as recognized by their elongated cell body morphology and expression of both GS or CRALBP, suggesting that the acquisition of a progenitor-like phenotype resulted from stimulated Müller cells.

Since the results of immunofluorescence assays indicated that $NaIO_3$ induces differentiation of Müller cells, western blotting was used to assess the PAX6 and SOX2 levels in control and damaged retinas. We observed a gradual increase in the expression of PAX6 and SOX2 at 6 h and 1 day PI, but the difference was not significant compared to controls. A significant increase was only observed at 3 and 7 days ($P < 0.05$) (**Figure 5H**). A significant decrease in the levels of PAX6 and SOX2 at 14 and 28 days was further confirmed by western blotting, which also demonstrated a significant decrease in the number of cells expressing PAX6 and SOX2 proteins in the retinas. Taken together, these results suggest that $NaIO_3$ precedes the activation of proneural factors involved in the differentiation of Müller cells.

Discussion

AMD is responsible for 8.7% of all blindness worldwide, and is the predominant cause of blindness in developed countries [13-16]. Similar to retinal dystrophies, Stargardt disease, and some forms of retinitis pigmentosa, AMD is characterized by degeneration of the photoreceptors and RPE in the human macula. For the last several decades, researchers focusing on novel therapies have employed the $NaIO_3$ model of retinal injury, which is induced by systemic injection of $NaIO_3$ [17]. The endogenous regeneration of the RPE can accompany pathologic conditions at low doses of $NaIO_3$ (15 mg/kg) [10]. However, the effect of high doses of $NaIO_3$ on endogenous Müller cell-derived progenitors and RPE regeneration is still unclear.

For several decades, we have known that fish and birds are capable of regenerating their neural retinas [18, 19]. Further, previous studies have shown that Müller cells have the capacity for retinal regeneration in chicks and rats [20, 21]. Using permanently labeled Müller cell-derived progenitors, it was demonstrated that these progenitors could produce all major retinal cell types and remain stably integrated into the retinal architecture [22, 23]. The regenerative capacity of the adult retina differs from species to species. In our study, we observed the transient activation of Müller cells, characterized by reprogramming and retinal regeneration during days 3-7 PI. SOX2 is a well-established neuronal stem cell-associated transcription factor responsible for controlling the self-renewal and differentiation of embryonic stem cells [24], the induction of somatic cells for the generation of induced pluripotent stem cells [25], the reprogramming of non-neuronal cells into neurons [26, 27], and the regulation of neural evolution [28, 29]. SOX2 expression was significantly increased in proliferating Müller glial cells in our study. Previous reports have demonstrated that SOX2 is required for the proliferation of Müller glia-derived neuronal progenitor cells and their potential to form a neuronal lineage, as well as for the optimal regeneration of photoreceptors [19]. PAX6, a paired domain and homeodomain-containing transcription factor, is one of the earliest genes expressed in the eye and is a pivotal regulatory gene in retinal and eye development. It plays an important role in retinal development in numerous nonvertebrate and vertebrate species [30, 31]. Here, we observed that PAX6 is expressed in Müller cell-derived progenitors, consistent with previous findings [32]. PAX6 contains multiple functional domains, and its upregulation in proliferating Müller cells as well as role in the formation of progenitors from Müller cells has been reported [33]. Thus, Müller glial cells represent a potential target for reprogramming strategies aimed at retinal repair.

In this study, we examined rat retinal tissue histology and morphology as a function of time after $NaIO_3$ injury, and demonstrated that RPE cell death started 6 hours PI. Kiuchi et al. showed that RPE cell necrosis was induced as early as 6 hours post-$NaIO_3$ treatment, followed by photoreceptor outer segment disruption and photoreceptor cell apoptosis after 24 hours [34]. Our analysis showed that RPE regeneration after $NaIO_3$ injury was present on day 3 and completed by day 7.

Machalińska et al concluded that complete regeneration of the RPE and considerable improvement of photoreceptor architecture by histologi cal assessment of retinas after 35 mg/kg $NaIO_3$ administration [12]. However, the precise mechanisms underlying RPE regeneration are not fully understood. The establishment of RPE regeneration is an important first step toward identifying factors that may improve regenerative approaches for AMD and related diseases. In the present study, we find that moderate acute retinal injury is accompanied by distinctive glial activation. Machalinska et al. showed that repair mechanisms within injured retinas involve a distinctive glial response. Glial cell proliferation and migration play active roles in RPE regeneration [10]. Müller glial cells, which are the only cell type to span all retinal layers, have processes that contact neighboring neurons and form part of the outer and inner limiting membranes [35, 36]. These cells provide the retina with biochemical and structural support, and contribute to its homeostasis and integrity [37, 38]. Accordingly, we speculate that Müller glial cells are the predominant active macroglial cells involved in supporting post-injury restoration of retinal homeostasis and biochemical support. Following the removal of cell debris by phagocytosis, involving both macrophages and Müller glia, the

remaining undamaged retinal cells begin to regenerate. Moreover, the expression of the stem and progenitor cell gene markers SOX2 and PAX6 in the limited number of GS- and CRALBP-positive cells is essential for retinal regeneration.

Conclusions

In summary, the findings presented in this study indicate that Müller cells express SOX2 and PAX6 under normal and pathologic conditions, and in particular, 3-7 days after $NaIO_3$ treatment. These findings suggest possible signaling pathways controlling Müller glia and RPE cell regeneration, but there is undoubtedly much more to learn about these remarkable cells. Our results pinpoint the fundamental importance of understanding the morphological, pathological, and molecular expression changes accompanying retinal damage, and may aid in the identification of possible therapeutic targets promoting retinal regeneration.

Acknowledgements

This work was supported by Stem cells therapy in ocular degenerative diseases (grant NO: 3D516D663429).

Disclosure of conflict of interest

None.

Abbreviations

$NaIO_3$, Sodium iodate; CRALBP, Cellular retinaldehyde-binding protein; GS, Glutamine synthetase; PAX6, Paired box 6; SOX2, SRY box 2; PCNA, Proliferating cell nuclear antigen; RPE, Retinal pigment epithelium; AMD, Age-related macular degeneration; VEGF, vascular endothelial growth factor; H&E, Hematoxylin and eosin; GCL, Ganglion cell layer; INL, Inner nuclear layer; ONL, Outer nuclear layer; IS/OS, Inner and outer segment.

Address correspondence to: Dr. Guanfang Su, Eye Center, The Second Hospital of Jilin University, 218 Ziqiang Street, Changchun 130021, Jilin, China. Tel: +86 43181136530; Fax: +86 43181136530; E-mail: lysu2015@163.com

References

[1] Lim LS, Mitchell P, Seddon JM, Holz FG and Wong TY. Age-related macular degeneration. Lancet 2012; 379: 1728-1738.

[2] Bressler NM, Doan QV, Varma R, Lee PP, Suner IJ, Dolan C, Danese MD, Yu E, Tran I and Colman S. Estimated cases of legal blindness and visual impairment avoided using ranibizumab for choroidal neovascularization: non-Hispanic white population in the United States with age-related macular degeneration. Arch Ophthalmol 2011; 129: 709-717.

[3] Varma R, Bressler NM, Doan QV, Danese M, Dolan CM, Lee A and Turpcu A. Visual impairment and blindness avoided with ranibizumab in hispanic and non-hispanic whites with diabetic macular edema in the United States. Ophthalmology 2015; 122: 982-989.

[4] Bressler SB, Ayala AR, Bressler NM, Melia M, Qin H, Ferris FL 3rd, Flaxel CJ, Friedman SM, Glassman AR, Jampol LM, Rauser ME; Diabetic Retinopathy Clinical Research Network. Persistent macular thickening after ranibizumab treatment for diabetic macular edema with vision impairment. JAMA Ophthalmol 2016; 134: 278-285.

[5] Webster SH, Rice ME, Highman B and Von Oettingen WF. The toxicology of potassium and sodium iodates: acute toxicity in mice. J Pharmacol Exp Ther 1957; 120: 171-178.

[6] Hanus J, Anderson C, Sarraf D, Ma J and Wang S. Retinal pigment epithelial cell necroptosis in response to sodium iodate. Cell Death Discov 2016; 2: 16054.

[7] Xia H, Krebs MP, Kaushal S and Scott EW. Enhanced retinal pigment epithelium regeneration after injury in MRL/MpJ mice. Exp Eye Res 2011; 93: 862-872.

[8] Franco LM, Zulliger R, Wolf-Schnurrbusch UE, Katagiri Y, Kaplan HJ, Wolf S and Enzmann V. Decreased visual function after patchy loss of retinal pigment epithelium induced by low-dose sodium iodate. Invest Ophthalmol Vis Sci 2009; 50: 4004-4010.

[9] Redfern WS, Storey S, Tse K, Hussain Q, Maung KP, Valentin JP, Ahmed G, Bigley A, Heathcote D and McKay JS. Evaluation of a convenient method of assessing rodent visual function in safety pharmacology studies: effects of sodium iodate on visual acuity and retinal morphology in albino and pigmented rats and mice. J Pharmacol Toxicol Methods 2011; 63: 102-114.

[10] Machalinska A, Kawa MP, Pius-Sadowska E, Roginska D, Klos P, Baumert B, Wiszniewska B and Machalinski B. Endogenous regeneration of damaged retinal pigment epithelium following low dose sodium iodate administration: an insight into the role of glial cells in retinal repair. Exp Eye Res 2013; 112: 68-78.

[11] Gong L, Wu Q, Song B, Lu B and Zhang Y. Differentiation of rat mesenchymal stem cells transplanted into the subretinal space of sodi-

um iodate-injected rats. Clin Exp Ophthalmol 2008; 36: 666-671.
[12] Machalinska A, Lejkowska R, Duchnik M, Kawa M, Roginska D, Wiszniewska B and Machalinski B. Dose-dependent retinal changes following sodium iodate administration: application of spectral-domain optical coherence tomography for monitoring of retinal injury and endogenous regeneration. Curr Eye Res 2014; 39: 1033-1041.
[13] Klein R, Klein BE and Cruickshanks KJ. The prevalence of age-related maculopathy by geographic region and ethnicity. Prog Retin Eye Res 1999; 18: 371-389.
[14] Klaver CC, Assink JJ, van Leeuwen R, Wolfs RC, Vingerling JR, Stijnen T, Hofman A and de Jong PT. Incidence and progression rates of age-related maculopathy: the rotterdam study. Invest Ophthalmol Vis Sci 2001; 42: 2237-2241.
[15] Kawasaki R, Yasuda M, Song SJ, Chen SJ, Jonas JB, Wang JJ, Mitchell P and Wong TY. The prevalence of age-related macular degeneration in Asians: a systematic review and meta-analysis. Ophthalmology 2010; 117: 921-927.
[16] Wong TY, Chakravarthy U, Klein R, Mitchell P, Zlateva G, Buggage R, Fahrbach K, Probst C and Sledge I. The natural history and prognosis of neovascular age-related macular degeneration: a systematic review of the literature and meta-analysis. Ophthalmology 2008; 115: 116-126.
[17] Noell WK. Experimentally induced toxic effects on structure and function of visual cells and pigment epithelium. Am J Ophthalmol 1953; 36: 103-116.
[18] Todd L, Suarez L, Quinn C and Fischer AJ. Retinoic acid-signaling regulates the proliferative and neurogenic capacity of Muller glia-derived progenitor cells in the avian retina. Stem Cells 2018; 36: 392-405.
[19] Gorsuch RA, Lahne M, Yarka CE, Petravick ME, Li J and Hyde DR. Sox2 regulates Muller glia reprogramming and proliferation in the regenerating zebrafish retina via Lin28 and Ascl1a. Exp Eye Res 2017; 161: 174-192.
[20] Gallina D, Palazzo I, Steffenson L, Todd L and Fischer AJ. Wnt/beta-catenin-signaling and the formation of Muller glia-derived progenitors in the chick retina. Dev Neurobiol 2016; 76: 983-1002.
[21] Karl MO, Hayes S, Nelson BR, Tan K, Buckingham B and Reh TA. Stimulation of neural regeneration in the mouse retina. Proc Natl Acad Sci U S A 2008; 105: 19508-19513.
[22] Fausett BV and Goldman D. A role for ALpha1 tubulin-expressing Muller glia in regeneration of the injured zebrafish retina. J Neurosci 2006; 26: 6303-6313.
[23] Ramachandran R, Reifler A, Parent JM and Goldman D. Conditional gene expression and lineage tracing of TUBA1A expressing cells during zebrafish development and retina regeneration. J Comp Neurol 2010; 518: 4196-4212.
[24] Kopp JL, Ormsbee BD, Desler M and Rizzino A. Small increases in the level of Sox2 trigger the differentiation of mouse embryonic stem cells. Stem Cells 2008; 26: 903-911.
[25] Takahashi K, Tanabe K, Ohnuki M, Narita M, Ichisaka T, Tomoda K and Yamanaka S. Induction of pluripotent stem cells from adult human fibroblasts by defined factors. Cell 2007; 131: 861-872.
[26] Karow M, Sanchez R, Schichor C, Masserdotti G, Ortega F, Heinrich C, Gascon S, Khan MA, Lie DC, Dellavalle A, Cossu G, Goldbrunner R, Gotz M and Berninger B. Reprogramming of pericyte-derived cells of the adult human brain into induced neuronal cells. Cell Stem Cell 2012; 11: 471-476.
[27] Heinrich C, Bergami M, Gascon S, Lepier A, Vigano F, Dimou L, Sutor B, Berninger B and Gotz M. Sox2-mediated conversion of NG2 glia into induced neurons in the injured adult cerebral cortex. Stem Cell Reports 2014; 3: 1000-1014.
[28] Okuda Y, Yoda H, Uchikawa M, Furutani-Seiki M, Takeda H, Kondoh H and Kamachi Y. Comparative genomic and expression analysis of group B1 sox genes in zebrafish indicates their diversification during vertebrate evolution. Dev Dyn 2006; 235: 811-825.
[29] Taranova OV, Magness ST, Fagan BM, Wu Y, Surzenko N, Hutton SR and Pevny LH. SOX2 is a dose-dependent regulator of retinal neural progenitor competence. Genes Dev 2006; 20: 1187-1202.
[30] Nornes S, Clarkson M, Mikkola I, Pedersen M, Bardsley A, Martinez JP, Krauss S and Johansen T. Zebrafish contains two pax6 genes involved in eye development. Mech Dev 1998; 77: 185-196.
[31] Xu S, Sunderland ME, Coles BL, Kam A, Holowacz T, Ashery-Padan R, Marquardt T, McInnes RR and van der Kooy D. The proliferation and expansion of retinal stem cells require functional Pax6. Dev Biol 2007; 304: 713-721.
[32] Raymond PA, Barthel LK, Bernardos RL and Perkowski JJ. Molecular characterization of retinal stem cells and their niches in adult zebrafish. BMC Dev Biol 2006; 6: 36.
[33] Zelinka CP, Volkov L, Goodman ZA, Todd L, Palazzo I, Bishop WA and Fischer AJ. mTor signaling is required for the formation of proliferating muller glia-derived progenitor cells in the chick retina. Development 2016; 143: 1859-1873.

[34] Kiuchi K, Yoshizawa K, Shikata N, Moriguchi K and Tsubura A. Morphologic characteristics of retinal degeneration induced by sodium iodate in mice. Curr Eye Res 2002; 25: 373-379.
[35] Reichenbach A and Reichelt W. Postnatal development of radial glial (Muller) cells of the rabbit retina. Neurosci Lett 1986; 71: 125-130.
[36] Magalhaes MM and Coimbra A. The rabbit retina Muller cell. A fine structural and cytochemical study. J Ultrastruct Res 1972; 39: 310-326.
[37] Reichenbach A and Bringmann A. New functions of Muller cells. Glia 2013; 61: 651-678.
[38] Bringmann A, Iandiev I, Pannicke T, Wurm A, Hollborn M, Wiedemann P, Osborne NN and Reichenbach A. Cellular signaling and factors involved in Muller cell gliosis: neuroprotective and detrimental effects. Prog Retin Eye Res 2009; 28: 423-451.